4TH INTERNATIONAL ROTATING EQUIPMENT CONFERENCE

2019 | 080

CAPM vs. Bulk Flow - reliable and efficient prediction of forces and leakage for annular gaps in pumps

PIF-centrifugal pumps - product lubricated bearing

Robin Matthias Robrecht, Technische Universität Darmstadt

Maximilian M. G. Kuhr, Technische Universität Darmstadt
Peter F. Pelz, Technische Universität Darmstadt

This paper has been presented and published on the occasion of the 4th International Rotating Equipment Conference 2019.

ABSTRACT

The interaction of rotor and casing is strongly influenced by the flow in annular gaps of pumps. State of the art in efficient prediction of forces and leakage at high Reynolds numbers are models based on the bulk flow theory (Childs, 1993). This bulk flow model omits viscous stress in the fluid and generally provides hydrodynamic variables only as sine/cosine functions over the gap circumference.

Motivated by the uncertainty of the predictions caused by these approximations, a more physical model was developed in recent works at TU Darmstadt. The CAPM (clearance averaged pressure model) takes into account viscous friction, both laminar and turbulent, by means of ansatz functions for velocity profiles. The only inherent assumption is constant pressure over the gap height due to the small ratio of mean gap height to the radius of the rotor. Axial and circumferential coordinates are treated differentially, the radial coordinate is treated with integrals over gap height. Thus, the solver for the model is based on a two dimensional finite differencing scheme solving the complete nonlinear continuity, axial and circumferential momentum equations via a SIMPLEC algorithm.

As yet, the implementation was validated extensively with hypothetical turbulent test cases by means of CFD (Lang, 2018). In the presented paper, suitable boundary conditions for the CAPM are described which allow for successful calculation of real application cases. Furthermore the CAPM is compared to a bulk flow model at typical operation conditions of media lubricated journal bearings where neither inertia nor viscous effects are negligible. Increasing differences of the predictions of the two models are seen for high eccentricities, high flow number and long annular gaps.

1 INTRODUCTION

The design of modern centrifugal pumps demands reliable and computational efficient prediction of leakage through narrow annular gaps and dynamic forces exerted by the fluid on the rotor [1]. Those annular gaps serve as bearings and equally as seals in a machine and govern both its energetic efficiency as well as dynamics and stability of the rotor. Despite the importance of the annular gap as machine element, there are no universally reliable and computational efficient models for flow in annular gaps up today. For this reason, a new model was developed recently – the CAPM (clearance averaged pressure model) [1].

For journal bearings, established models are usually based on fluid film lubrication theory by Osborne Reynolds, 1886 [2]. The so called Reynolds equation omits the nonlinear convective momentum terms and thus inherently is valid only for flow with negligible inertia. For annular gaps on the other hand, models mostly are based on bulk flow theory by Hirs, established 1973 [3]. In practice, the model of Childs is commonly used [4, 5]. Viscous stresses in the fluid film are omitted completely and wall shear stress is modeled with friction factor laws. Furthermore the influence of eccentricity is considered by linear perturbation theory, circumferential distribution of variables are provided by sine/cosine functions. Those assumptions generally only hold for high Reynolds number and small eccentricity.

Figure 1 shows a sectional view of a centrifugal pump. Note that all dimensional quantities in this paper are denoted with a tilde, corresponding non-dimensional counterparts without. For the definitions of non-dimensional quantities refer to chapter 6. The shaft rotates with rotational speed $\tilde{\Omega}$. Volume flow is denoted by $\tilde{Q}$ and indicated by the arrows. Due to the pressure difference $\Delta\tilde{p} = \tilde{p}_2 - \tilde{p}_1$, the process fluid is channeled from the impeller outlet through two narrow annular gaps, so called media lubricated journal bearings. The fluid then returns to the impeller inlet through the hollow shaft. Operation conditions in media lubricated journal bearings are such, that neither inertia nor viscous stresses in the fluid are negligible. Eccentricity ratios of $\varepsilon \geq 0.9$ are common. Flow usually is fully turbulent but could occasionally be laminar as well.

For design and calculation purposes either the pressure difference over the gap $\Delta\tilde{p}$ is given and the (leakage) volume flow $\tilde{Q}$ is unknown or the volume flow is given and the pressure difference is unknown. Resulting forces on the rotor $\tilde{F}$ are obtained by integrating the calculated pressure field and wall shear stress over the rotor surface.

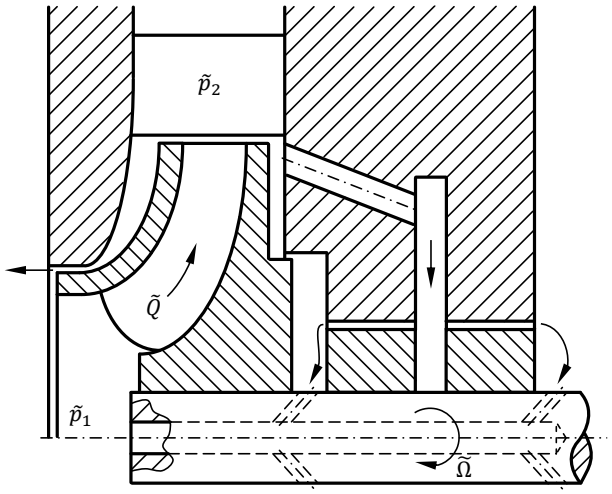

Figure 1. Schematic sectional view of a centrifugal pump impeller supported by process media lubricated journal bearings.

2 CAPM GOVERNING EQUATIONS AND BOUNDARY CONDITIONS

The CAPM comprises an integro-differential approach for incompressible and isothermal flow through a cylindrical plain annular gap without occurrence of cavitation. The model geometry is depicted in figure 2. The rotor has the radius $\tilde{R}$ and rotational speed $\tilde{\Omega}$. The dynamics of the rotor are considered by an orbital motion with frequency $\tilde{\omega}$ around the bearing centerline with eccentricity $\tilde{\varepsilon}$. Additionally the rotor can be tilted with angle γ. The bearing has the length $\tilde{L}$. The gap with variable gap height $\tilde{h}$ is filled with fluid of kinematic viscosity $\tilde{\nu}$. The fluid enters the gap with mean axial velocity $\tilde{\bar{C}}_z$ and circumferential velocity $\tilde{\bar{C}}_{\varphi,0}$. Time dependency of the variables is eliminated by use of a rotating coordinate system. Due to the order of magnitude $\psi \sim 10^{-3}$, the radial velocity component and radial pressure gradient are negligible. The considered control volume extends over the complete gap height and infinitesimal segments in axial and circumferential direction.

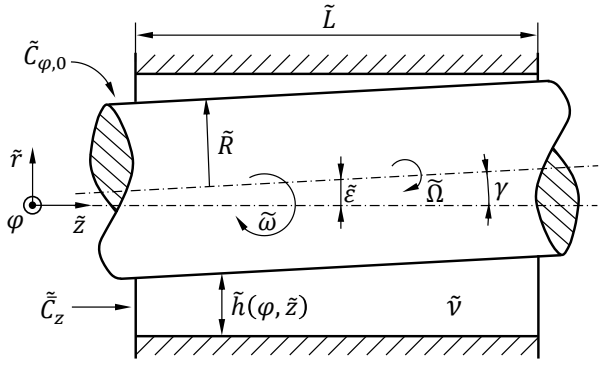

Figure 2. Generic model geometry of a plain annular gap for the CAPM.

For steady state, continuity equation, angular and axial momentum equation for this control volume in non-dimensional form read

$$\frac{\partial}{\partial\varphi}h\int_0^1 w_\varphi \,\mathrm{d}y + \frac{\phi}{L}\frac{\partial}{\partial z}h\int_0^1 c_z \,\mathrm{d}y = 0, \tag{1}$$

$$\frac{\partial}{\partial\varphi}h\int_0^1 w_\varphi^2 \,\mathrm{d}y + \frac{\phi}{L}\frac{\partial}{\partial z}h\int_0^1 w_\varphi c_z \,\mathrm{d}y = -\frac{h}{2}\frac{\partial p}{\partial\varphi} + \frac{\tau_{\mathrm{Stat},\varphi} - \tau_{\mathrm{Rot},\varphi}}{2\psi} \text{ and} \tag{2}$$

$$\phi\frac{\partial}{\partial\varphi}h\int_0^1 w_\varphi c_z \,\mathrm{d}y + \frac{\phi^2}{L}\frac{\partial}{\partial z}h\int_0^1 c_z^2 \,\mathrm{d}y = -\frac{h}{2L}\frac{\partial p}{\partial z} + \frac{\tau_{\mathrm{Stat},z} - \tau_{\mathrm{Rot},z}}{2\psi}. \tag{3}$$

This system of coupled partial differential equations is solved numerically taking into account for non-linear convective terms. The integrals are solved analytically by use of power law ansatz functions for velocity profiles over gap height. Wall shear stress for turbulent flow is accounted for by the use of friction factors similarly to bulk flow theory. Further details to the derivation and solving algorithms of the governing equations can be found in the work of Lang [1].

Besides the governing equations, the formulation of sensible boundary conditions are an absolute requirement for a meaningful solution. Although a fact well known, it is often overlooked in physical modelling and even use of CFD. In case of a narrow annular gap, conditions at the outlet can be defined easily while the conditions at the inlet are usually unknown and require a more complex approach.

At the inlet, a pressure loss due to inertia effects in the fluid is well documented [6]. The occurrence of this pressure loss is named after Lomakin, who first described it [7]. In fact, the Lomakin effect is nothing else than a pressure loss caused by an abrupt contraction of the flow cross section. In detail, the flow separates at the sharp edge of the inlet as a result of fluid inertia. The resulting separation bubble narrows the flow cross section even more. Hereafter the flow expands to the cross section defined by geometry and the pressure loss can be described by a Carnot shock.

For potential flow around a static and concentric shaft, i.e. $\tilde{\varepsilon}, \widetilde{\Omega} = 0$, the pressure loss coefficient can be derived analytically with use of the hodograph method to $\zeta = 0.41$ [8, 9]. In practice, a value of $\zeta \approx 0.5$ is often used [10]. Generally, the inlet pressure loss coefficient will depend on inlet geometry, rotor dynamics and flow conditions: $\zeta = \zeta(\psi, \varepsilon, \omega, Re, \phi)$. Because of the mostly empirical character accredited to the pressure loss coefficient, it is usually assumed to be constant in circumference. A constant coefficient will already provide a basis for modelling the Lomakin effect and pressure loss will vary in circumference.

However, Kündig not only observed a circumferential distribution of the inlet pressure losses but also of the pressure loss coefficient itself in his experiments [10]. He attributes this effect to a rounded inlet edge which prevents flow separation at the narrow part of the gap. Moreover, experience suggests a general dependence of the inlet loss coefficient of circumference though, even for sharp edges. Therefore, the authors state the hypotheses that

$$\zeta = \zeta(\varphi), \tag{4}$$

which establishes a way to a more physical modelling approach. Hence, the formulation for inlet pressure loss used by the CAPM reads

$$\Delta p = \left\{\; p(\varphi) + [1 + \zeta(\varphi)]\left[\phi^2 C_z^2(\varphi) + C_\varphi^2(\varphi)\right] \;\right\}_{z=0}. \tag{5}$$

Equation (5) couples velocity and pressure distribution at the inlet either by given pressure difference Δp or flow number ϕ. Due to conservation of angular momentum, C_φ is assumed to be constant at inlet.

At the outlet, a Neumann boundary condition for velocity is used. The gradient in normal direction is zero, such that the velocity field at the boundary develops out of the calculation domain. The stress vector has to be continuous $\vec{t}_{(\vec{n})} = -\vec{t}_{(-\vec{n})}$ on the surface of the free stream emanating from the gap. The pressure gradient in the free stream is negligible, thus the pressure at outlet is constant and is provided as Dirichlet boundary condition.

In bulk flow theory, it is often referred to a pressure recovery factor at the outlet. It can be modelled with stream filament theory and pressure loss terms, likewise to entrance losses mentioned above [5]. However, a corresponding formulation is applicable only for very specific conditions and not for plenum type outlets at all.

Figure 3 shows results of the CAPM in comparison with a bulk flow model (Childs 1993, [5]), Reynolds equation and experimental results. Further measurements, a detailed description of the test rig, measurement procedure as well as uncertainty can be found in the work of Kuhr [11]. Operation

conditions resemble a typical use case of process media lubricated journal bearings. Results shown are at static eccentricity and without tilt ($\gamma, \omega = 0$).

The force predictions of the CAPM meet the experimental results very well in the whole eccentricity range. For $\varepsilon \leq 0.6$ a constant value of $\zeta = 0.5$ is used in accordance with the analytical value mentioned above. For $\varepsilon > 0.6$ the sine distribution of $\zeta(\varphi, \varepsilon)$ shown in figure 4 was used, which in the first run was found empirically. A physical model for the pressure loss coefficient $\zeta(\varphi, \varepsilon)$ is currently developed on grounds of these promising results.

Predictions of the bulk flow model meet the experimental results well for $\varepsilon \leq 0.6$ as expected for the linearized 1D-model. Due to the model's nature, only a constant value of $\zeta = 0.5$ could be used for calculation. For the bulk flow model as well as for the CAPM a friction factor model of Blasius used with the same coefficients. The friction coefficients were calibrated for hydraulic smooth walls by Lang [1]. The numerically solved 2D Reynolds equation predicts force much too low in the whole eccentricity range. Though not limited to a linear curve, the slope of the measurements is also not represented well in a qualitative way. Omission of convective terms and inlet pressure loss obviously result in unfit prediction of resulting force. Compensation of model insufficiencies with turbulence factors for the Reynolds equation seems futile in consideration of the shown discrepancies.

3 CAPM VS. BULK FLOW

Figure 3 shows good accordance of both the CAPM and the bulk flow model with experimental results for a moderate eccentricity range. In this section the two models will be compared for further operation conditions.

Inspectional dimensional analysis shows that forces of inertia in the fluid scale with ψRe. For $\psi Re \gg 1$ the assumption of bulk velocity is valid. When $\psi Re \sim 1$ viscous forces and forces of inertia are of the same order of magnitude and neither can be neglected. While maintaining turbulent flow ($Re' > 2300$ [12]), the bulk flow model is assumed to deviate more from the CAPM for reasonable low values of ψRe. Both models don't consider development of axial boundary layers, even though Lang pointed out that for $Re^* \sim 1$ it is an important influence [13]. For the CAPM, consideration of boundary layer development is possible in principle while it is impossible for the bulk flow model.

As described earlier, both models rely on the same friction factor definition and corresponding coefficients. For direct comparison both models use constant $\zeta = 0.5$. Inlet circumferential velocity $C_{\varphi,0} = 0.5$ and $\gamma, \omega = 0$ again. For the following results, the inertia parameter ψRe, flow number ϕ and the gap length L were varied in both models and results compared.

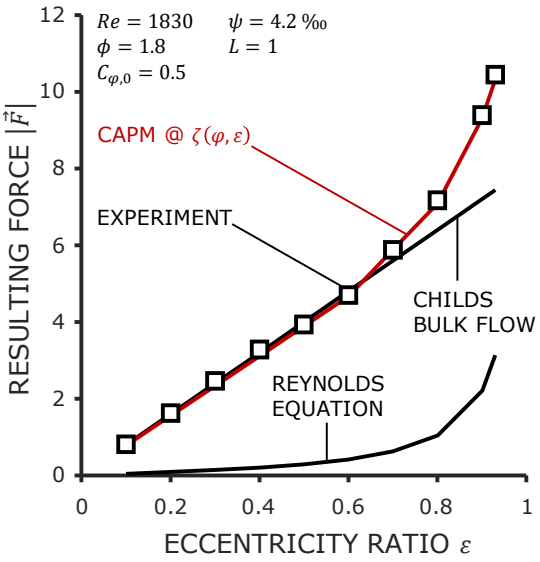

Figure 3. CAPM, bulk flow model and Reynolds equation versus experiment ($\psi Re = 7.7$, $Re^* = 13.9$, $Re' = 5440$).

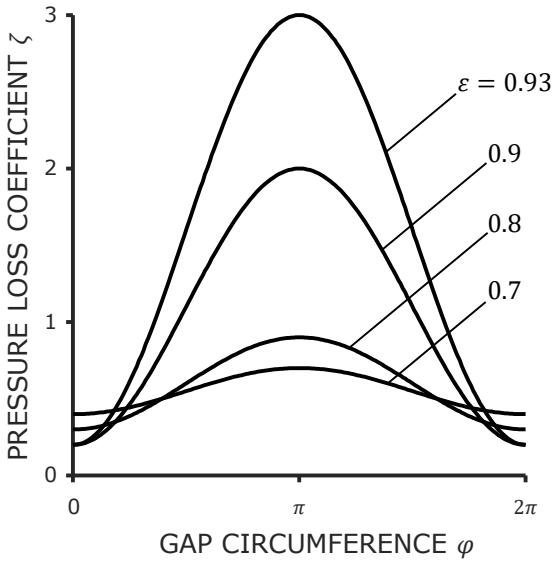

Figure 4. Assumed circumferential distribution of the inlet pressure loss coefficient for the CAPM due to the Lomakin effect for different eccentricities.

Each diagram in figure 5 shows force predictions over eccentricity ratio of the CAPM and the bulk flow model for $\phi = 1$ and 5. Obviously, the flow number is an important parameter contributing to the resulting force on the rotor. Thus, the resulting force is greater overall and the slope with ε is generally steeper for most parameter pairings. In diagrams c) and d) the slopes of the curves of the two models seem to differ more with higher flow number. As mentioned above, the bulk flow model only predicts constant change of force with eccentricity due to use of linear perturbation theory. The predictions of the CAPM can be assumed to represent a more physical correlation, as hinted to by figure 3. In diagram a) and b) the graphs of the CAPM differ qualitatively for $\phi = 5$. All other graphs show a progressive distribution with ε while the one mentioned in diagram a) has a declining slope. The graph mentioned in diagram b) has a slope varying slightly from declining to progressive.

The resulting force is generally decreasing with increase of ψRe for both models as shown in diagram d). Assuming $Re = \text{const.}$, the increase can be attributed to ψ alone. Of course a wider gap yields a smaller pressure in the fluid film and thus a smaller resulting force. Assuming $\psi = \text{const.}$, the resulting force decreases with increasing Re. The physical cause of this behaviour can be attributed to the so called Bernoulli effect (effect of circumferential inertia), which reduces pressure within the fluid film at the narrower parts of the gap. Therefore it is easy to understand the reduction in resulting force at high eccentricity or high Reynolds number. Similar behaviour can be seen as well in experiments for hydrostatic/hybrid journal bearings at high eccentricities, e.g. in [14].

The resulting forces of the bulk flow model increase at $\phi = 1$ and decrease slightly at $\phi = 5$ with increasing L. The predictions of the CAPM seem to

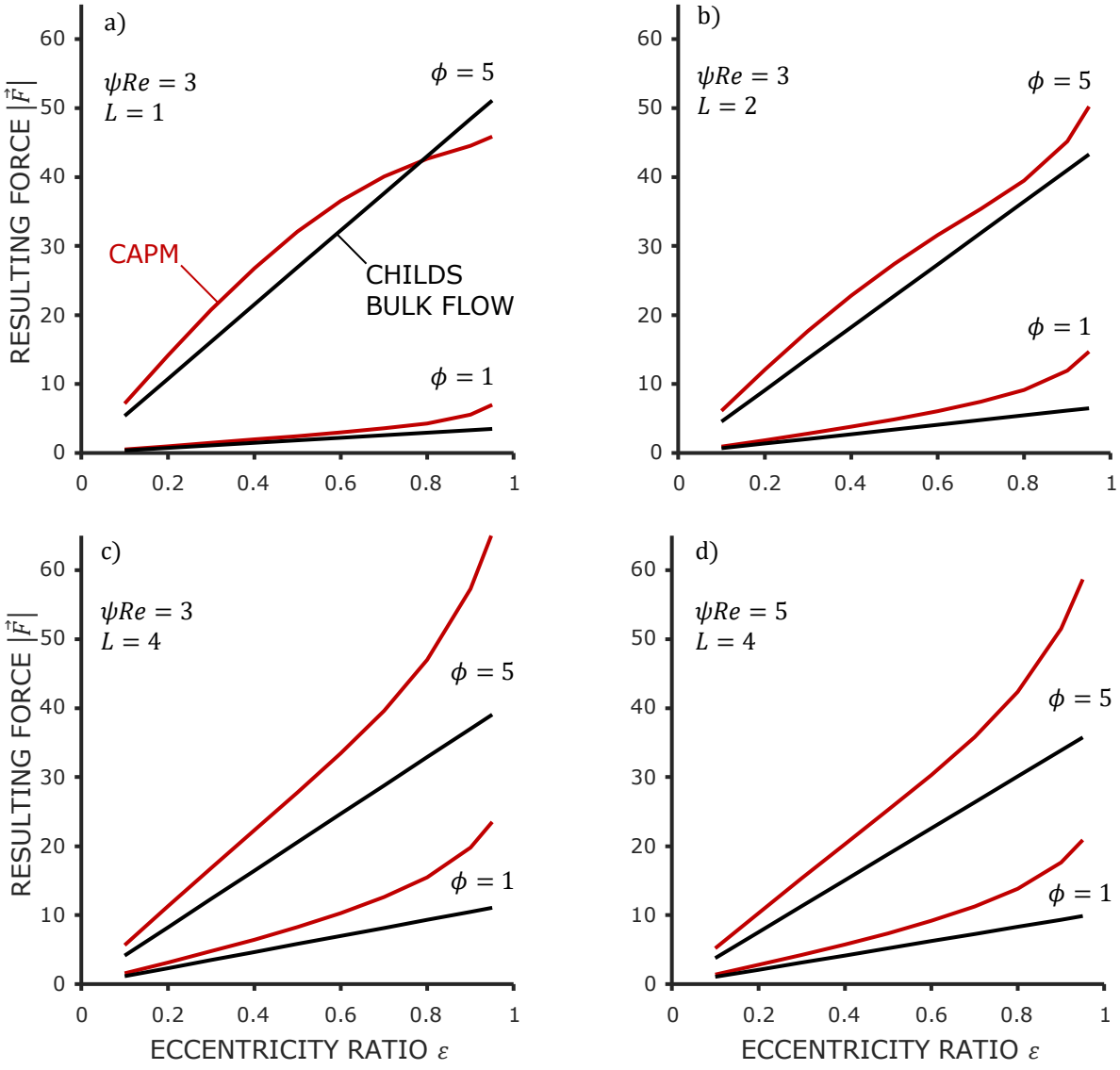

Figure 5. Comparison of force over eccentricity for the CAPM and the bulk flow model. Diagrams a), b) and c) show results for $\psi Re = 3$ and $L = 1,2,4$. Diagram d) shows results for $\psi Re = 5$ and $L = 4$.

generally increase with L, although it is difficult to define with the qualitative difference in the curves. Generally, the same behaviour described above for $\psi Re = 3$ is seen for $L = 1{,}2$ at $\psi Re = 5$ as well. Thus, the corresponding diagrams are not shown.

4 CONCLUSIONS

With the CAPM a new approach for computational efficient and reliable prediction of dynamic forces and leakage in annular gaps was created. With the use of suitably modelled boundary conditions it can represent a new means of machine design fit for modern requirements of process media lubricated journal bearings. The inlet boundary condition has to take into account pressure losses commonly referred to as Lomakin effect. The pressure loss coefficient is assumed to be a distribution in circumference and a physically motivated model will be derived in the future. Experiments suggest validity of the statements mentioned above. Furthermore the CAPM was compared with a bulk flow model. The results show larger discrepancy in force prediction of the bulk flow model for large eccentricities, higher flow number and longer gaps for operation conditions typical for media lubricated journal bearings. The force predictions of the bulk flow model are up to $\approx 60\ \%$ lower than the CAPM. Further comparison of the two models with variation of inlet circumferential velocity $C_{\varphi,0}$ and orbit frequency ω are projected. Calculation results will be consolidated with measurements in the future.

5 ACKNOWLEDGEMENTS

The presented results were obtained within the research project “Fördermediengeschmierte Gleitlager in Pumpen”, project No. 19225 BG/2, funded by the programme for promoting the Industrial Collective Research (IGF) of the German Ministry of Economic Affairs and Energy (BMWi), approved by the Arbeitsgemeinschaft industrieller Forschungsvereinigungen “Otto von Guericke” e.V. (AiF). We want to thank all the participants of the working group for the constructive and close collaboration.

6 DEFINITIONS

relative gap width	$\psi \coloneqq \tilde{\bar{h}}/\tilde{R}$
relative gap length	$L \coloneqq \tilde{L}/\tilde{R}$
relative circumferential velocity at inlet	$C_{\varphi,0} \coloneqq \tilde{C}_{\varphi,0}/\tilde{\Omega}\tilde{R}$
mean axial velocity in m/s	$\tilde{\bar{C}}_z \coloneqq \dfrac{\tilde{Q}}{2\pi\tilde{R}\tilde{\bar{h}}}$
flow number	$\phi \coloneqq \tilde{\bar{C}}_z/\tilde{\Omega}\tilde{R}$
Reynolds number	$Re \coloneqq \dfrac{\tilde{\Omega}\tilde{R}\tilde{\bar{h}}}{\tilde{\nu}}$
modified Reynolds number	$Re' \coloneqq Re\sqrt{1+\phi^2}$
modified Reynolds number	$Re^* \coloneqq \dfrac{\phi}{L}\psi Re$
eccentricity ratio	$\varepsilon \coloneqq \tilde{\varepsilon}/\tilde{\bar{h}}$
relative orbit frequency	$\omega \coloneqq \tilde{\omega}/\tilde{\Omega}$
non-dimensional force	$F \coloneqq 2\tilde{F}/(\varrho\tilde{\Omega}^2\tilde{R}^3\tilde{L})$
non-dimensional pressure difference	$\Delta p \coloneqq 2\Delta\tilde{p}/(\varrho\tilde{\Omega}^2\tilde{R}^2)$

7 REFERENCES AND BIBLIOGRAPHY

[1] Lang, S.: *Effiziente Berechnung von Gleitlagern und Dichtspalten in Turbomaschinen*. Dissertation, Technische Universität Darmstadt, 2017. Aachen: Shaker Verlag 2018

[2] Reynolds, O.: *On the theory of lubrication and its application to Mr. Beauchamp Tower's experiments, including an experimental determination of the viscosity of olive oil.* PHILOSOPHICAL TRANSACTIONS OF THE ROYAL SOCIETY OF LONDON 177 (1886), S. 157–234

[3] Hirs, G. G.: *A Bulk-Flow Theory for Turbulence in Lubricant Films.* JOURNAL OF LUBRICATION TECHNOLOGY 95 (1973) 2, S. 137

[4] Childs, D. W.: *Finite-Length Solutions for Rotordynamic Coefficients of Turbulent Annular Seals.* JOURNAL OF LUBRICATION TECHNOLOGY 105 (1983) 3, S. 437

[5] Childs, D. W.: *Turbomachinery rotordynamics*. Phenomena, modeling, and analysis. New York: Wiley 1993

[6] Brennen, C. E.: *Hydrodynamics of pumps*. Cambridge: Cambridge University Press 2011

[7] Lomakin, A. A.: *Calculation of the critical speed and the conditions to ensure dynamic stability of the rotors in high pressure hydraulic machines, taking account of the forces in the seals (in Russian).* ENERGOMASHINOSTROENIE 14 (1958) 4

[8] Spurk, J. H. u. Aksel, N.: *Strömungslehre*. Einführung in die Theorie der Strömungen. Berlin: Springer 2010

[9] Spurk, J. H.: *Aufgaben zur Strömungslehre*. Springer-Lehrbuch. Berlin, Heidelberg, s.l.: Springer Berlin Heidelberg 1996

[10] Kündig, P.: *Gestufte Labyrinthdichtungen hydraulischer Maschinen*. Experimentelle Untersuchung der Leckage, der Reibung und der stationären Kräfte, ETH Dissertation. Zürich 1994

[11] Kuhr, M. G. M. u. Robrecht, R. M., Pelz, P. F.: *Measuring and simulation of fluid forces in annular gaps - Generic experiments covering the relevant parameter range for turbulent and laminar flow in pumps*. In: Pump Users International Forum 2019. 4th International Rotating Equipment Conference. Proceedings. 2019

[12] Szeri, A. Z.: *Fluid film lubrication*. Theory and design. Cambridge: Cambridge Univ. Press 2005

[13] Lang, S. u. Pelz, P. F.: *Unified Prediction of Hydrodynamic Forces in Plain Annular Seals and Journal Bearings by means of an Analytically Derived Design Tool*. In: Pump Users International Forum 2016. 3rd International Rotating Equipment Conference. Proceedings. Frankfurt am Main: Pumps + Systems Association within VDMA e.V 2016

[14] Xu, S.: *Experimental Investigation of Hybrid Bearings.* TRIBOLOGY TRANSACTIONS 37 (1994) 2, S. 285–292